Received: 24 April 2022 | Revised: 19 July 2022 | Accepted: 28 August 2022

DOI: 10.1002/cjce.24764

RESEARCH ARTICLE

THE CANADIAN JOURNAL OF CHEMICAL ENGINEERING

An LSTM-based mixed-integer model predictive control for irrigation scheduling

Bernard T. Agyeman | **Soumya R. Sahoo** | **Jinfeng Liu** | **Sirish L. Shah**

Department of Chemical & Materials Engineering, University of Alberta, Edmonton, Alberta, Canada

Correspondence
Jinfeng Liu, Department of Chemical & Materials Engineering, University of Alberta, Edmonton, AB, Canada.
Email: jinfeng@ualberta.ca

Funding information
Alberta Innovates; Natural Sciences and Engineering Research Council of Canada

Abstract

The development of well-devised irrigation scheduling methods is desirable from the perspectives of plant quality and water conservation. Accordingly, in this article, a mixed-integer model predictive control system is proposed to address the daily irrigation scheduling problem. In this framework, a long short-term memory (LSTM) model of the soil–crop–atmosphere system is employed to evaluate the objective of ensuring optimal water uptake in crops while minimizing total water consumption and irrigation costs. To enhance the computational efficiency of the proposed method, a heuristic method involving the logistic sigmoid function is used to approximate the binary variable that arises in the mixed-integer formulation. Through computer simulations, the proposed scheduler is applied to homogeneous and spatially variable fields. The results of these simulation experiments reveal that the proposed method can prescribe optimal/near-optimal irrigation schedules that are typical of irrigation practice within practical computational budgets.

KEYWORDS

mixed-integer MPC, sigmoid function, spatially variable irrigation scheduling

1 | INTRODUCTION

Agriculture accounts for about 70% of global freshwater withdrawals, the vast majority of which is used for irrigation purposes.[1] At the same time, the global water scarcity crisis is worsening due to increased stress on freshwater resources resulting from population growth and climate change. Given the rising freshwater shortages, there is a pressing need for precise irrigation management strategies that will guarantee sustainable water use while ensuring optimal plant development.

While irrigation guarantees favourable plant growth in areas where rainfall is insufficient, it is beneficial to irrigate to meet the specific water requirements of plants at the right time instant. This can be achieved by implementing well-devised irrigation control and scheduling operations on an hourly or daily basis for a planning horizon of usually up to a few hours, days, or weeks.[2] Traditionally, most control and scheduling operations in irrigation management are implemented in an open-loop fashion, where there is no direct connection between the supplied irrigation rate and the prevailing soil water status. However, open-loop implementations are known to be imprecise and do not guarantee optimal plant yield and enhanced water use efficiency. Precision irrigation methods have been advocated as a means of mitigating the defects associated with open-loop irrigation operations. In the context of systems engineering, precision irrigation can be realized by closing the irrigation decision-making loop to form a closed-loop system.[3]

Abbreviations: BDF, backward differentiation formula; LSTM, long short-term memory; MAE, mean absolute error; MPC, model predictive control; MSE, mean squared error; MZ, management zones.

Irrigation scheduling seeks to provide crops with the right amount of water at the appropriate times. To obtain precise and robust irrigation schedulers, models that capture the dynamics of the soil–crop–atmosphere system (agro-hydrological models) have been used to determine irrigation schedules. For example, Lopes et al.[4] transformed the scheduling problem into an optimal control problem to minimize the total irrigation volume. This optimal control problem relied on a soil water balance model. Similarly, Park et al.[5] used the one-dimensional (1D) Richards equation to develop a model predictive control (MPC) system that provided irrigation schedules for a centre pivot irrigation system. While these approaches were largely successful, the use of mechanistic models, also known as first principle models, in these methods has several practical drawbacks. Generally, mechanistic models are difficult to handle from a numerical point of view, and hence they render model-based scheduling schemes computationally inefficient. Furthermore, mechanistic models require time-consuming calibrations during their development.

Several studies have examined the use of statistical or data-driven models, also known as black box models, in irrigation scheduling. For instance, Nahar et al.[6] identified a linear parameter varying (LPV) model for a closed-loop scheduler and controller using input and output data obtained from the 1D Richards equation. Similarly, neural network models have been used to predict the dynamics of soil moisture due to their capacity to model nonlinear relationships between inputs and outputs. In the works of Capraro et al., Tsang and Jim, and Gu et al.,[7–9] irrigation schedules were determined based on soil moisture predictions from a feedforward neural network. Feedforward neural networks are generally unable to accurately model dynamic data due to their inability to preserve past information. Therefore, when these networks are applied to highly causal systems, such as agro-hydrological systems, they result in suboptimal predictions.[10] Recurrent neural networks (RNNs) are a robust type of neural network that are specifically designed to handle sequential data. Because of their internal memory, they can remember information from previous time steps, which allow them to be very accurate in modelling dynamic data. Theoretically, RNNs can be trained to solve problems that require learning long-term temporal dependencies. However, in practice, they are unable to learn such long-term dependencies due to the vanishing/exploding gradient problem. Long short-term memory (LSTM) networks are a special kind of RNN that are capable of learning long-term temporal dependencies and they have been successfully applied to nonlinear dynamical systems. In the context of irrigation scheduling, Adeyemi et al.[11] developed an LSTM model for the prediction of soil moisture content. The predictions from the identified model were used to determine the daily irrigation amount and the timing of the irrigation event.

Optimal control approaches have been applied to schedule irrigation. In this context, optimal control methods determine the control variables, specifically the water application depth and the irrigation time, that optimize some performance measure. For example, in the works of Rao et al. and Naadimuthu et al.,[12,13] irrigation was scheduled using the dynamic programming method to maximize crop yield. Although the dynamic programming approach has the advantage of being simple for unconstrained linear systems with a small state dimension, it suffers from the 'curse of dimensionality' (i.e., the size of the search space grows exponentially with the number of state variables), which limits its practical application in irrigation scheduling. MPC is regarded as an effective means of implementing the dynamic programming solution.[14] MPC relies on a sufficiently descriptive model of a system to optimize some performance measures and ensure constraint satisfaction. In an MPC scheme, at each sampling time instant, a finite horizon optimal control problem is solved in which the initial state is chosen as the current state of the system. This optimization yields a finite control sequence and the first control action is applied to the system. This is repeated at each sampling time instant with a receding prediction horizon. In the area of irrigation scheduling and control, McCarthy et al.[15] used MPC to determine irrigation timing and site-specific irrigation volumes. Similarly, in Delgoda et al.,[16] irrigation was scheduled using MPC to minimize root zone soil moisture deficit and total irrigation volume. In these studies, the MPCs were designed to maintain the root zone soil moisture at a predetermined set-point. The stability and the feasibility of a set-point tracking MPC are dependent on the desired set-point such that when there is a change in the desired set-point, these properties of the MPC may be lost. This demands a redesign of a set-point MPC at each change of set-point. The computational burden associated with this design makes a set-point tracking MPC less viable from a computational point of view. To ensure optimal growth of plants, it is sufficient to keep soil moisture content within a range/zone. Usually, the upper bound of the desired range is a point below the field capacity, and the lower bound is a point above the permanent wilting point of the soil under consideration. A MPC with zone objectives (zone control) is thus a natural choice for irrigation scheduling. In the context of irrigation scheduling, Nahar et al.[6] developed a closed-loop irrigation scheduling using a zone MPC.

Machine learning techniques have been successfully employed in recent works in the design and implementation

of model predictive controllers. For example, in the work of Wu et al.,[17] an MPC system was designed for nonlinear processes that utilize an ensemble of RNNs to predict their dynamics. In the work by Wu et al.,[18] an LSTM model was trained with sensor data corrupted with noise, and the resulting model was used to design a model predictive controller. In the work by Zhao et al.,[19] an MPC scheme for nonlinear systems was designed using autoencoder-based reduced-order machine learning models.

Scheduling problems are inherently combinatorial because the allocation of scarce resources to competing tasks over time involves many discrete decisions.[20] When irrigation is to be scheduled daily, the determination of the irrigation time (i.e., days on which the irrigation event should be performed) reduces to a discrete decision of whether or not the irrigation event should be performed on the days that make up the planning horizon. Thus, the daily irrigation scheduling problem can be transformed into an optimal control problem with both continuous—(irrigation volume, depth, or rate) and integer—(irrigation time) valued control variables. The early literature on MPC focused almost entirely on continuous-valued controls because of the computational difficulty associated with discrete decision variables.[21] With improvements in optimization software and computing performance, discrete-valued controls can be selected optimally by directly including them in the MPC design. The incorporation of discrete decision variables into the MPC formulation leaves its structure unchanged and any result that holds for the standard MPC holds also for MPC with discrete-valued control variables.[14]

Motivated by the above, this work develops an irrigation scheduler in the framework of a mixed-integer MPC with zone control for agro-hydrological systems that utilize an LSTM model to predict the dynamics of soil moisture. More specifically, the LSTM model is first developed based on a dataset generated from extensive open-loop simulations of a mechanistic agro-hydrological model. Subsequently, a mixed-integer MPC with zone objectives is developed based on the identified LSTM model. The proposed irrigation scheduler calculates the irrigation time and the irrigation rate that ensure optimal root water uptake while minimizing irrigation costs and total water consumption. Due to the inherently complex nature of mixed-integer programs, this work adopts a heuristic method that can be used to simplify the mixed-integer MPC to enhance the computational efficiency of the proposed scheduler. The main contributions of this work include:

1. A method to identify an LSTM model for the prediction of soil moisture content in an agro-hydrological system for both uniform and spatially variable fields.
2. A detailed closed-loop irrigation scheduler design in the framework of a mixed-integer MPC with zone control that ensures optimal root water uptake while minimizing irrigation costs and total water consumption. This work proposes separate designs for uniform and spatially variable fields. In the context of irrigation scheduling in spatially variable fields, designs that are tailored to small- and large-scale fields are also developed.
3. Extensive simulations that investigate the performance of the proposed scheduler.

Elements of the work presented in this paper were reported in the work of Agyeman et al.[22] Compared with that work,[22] this article presents detailed explanations, a comprehensive set of results, and it introduces a new set of results for irrigation scheduling in small- and large-scale spatially variable fields.

2 | PRELIMINARIES

In this section, we first describe the soil–crop–atmosphere system and introduce a mechanistic equation that can be used to model the soil moisture dynamics in an agro-hydrological system. This section concludes with a theoretical background on LSTMs.

2.1 | Agro-hydrological system

An agro-hydrological system characterizes the movement of water between the soil, crops, and the atmosphere. Figure 1 provides a simple illustration of an agro-hydrological system. In this system, water transport takes place primarily through irrigation, precipitation, evaporation, transpiration, infiltration, root water extraction, surface run-off, and drainage. The transport of water in the soil under the action of capillary and gravitational forces can be modelled using the Richards equation. Models that describe the dynamics of soil moisture, such as the Richards equation, are the most used tools for irrigation scheduling since water available for uptake by crops can be inferred from soil moisture.[24] The Richards equation can be expressed in capillary pressure head form as:

$$c(\psi)\frac{\partial \psi}{\partial t} = \nabla.\ (K(\psi)\nabla(\psi + z)) - S(\psi, z). \tag{1}$$

In Equation (1), ψ is the capillary pressure head (m), which describes the status of water in soil, t represents time (s), z is the spatial coordinate (m), $K(\psi)$ is the

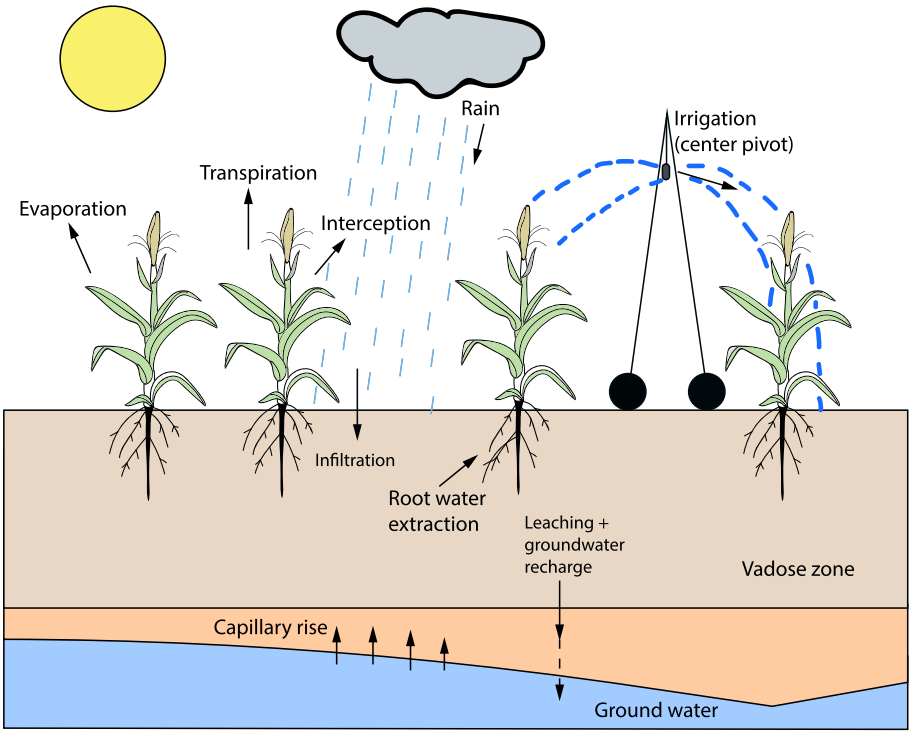

FIGURE 1 An agro-hydrological system[23]

unsaturated hydraulic water conductivity (ms^{-1}), and $c(\psi)$ is the capillary capacity (m^{-1}). $K(\psi)$ and $c(\psi)$ are parameterized by models of Mualem[25] and van Genuchten.[26] $K(\psi)$ and $c(\psi)$ rely on empirical parameters, namely, the saturated water content (θ_s), the residual water content (θ_r), the saturated hydraulic conductivity (K_s), and the curve fitting soil hydraulic parameters (α and n). These empirical hydraulic parameters are characteristics of the soil under consideration. $S(\psi, z)$ denotes the sink term ($m^3\ m^{-3}\ s^{-1}$) and it is expressed as:

$$S(\psi, z) = \rho(\psi)\mathcal{R}\left(K^c, ET^0, z_r\right) \tag{2}$$

where $\rho(\psi)$ is a dimensionless stress water factor and $\mathcal{R}(\cdot)$ is the root water uptake model, which is a function of the crop coefficient K^c (dimensionless), the reference evapotranspiration ET^0 (ms^{-1}), and the rooting depth z_r (m).

2.2 | LSTM network

LSTMs are a special kind of RNN that are capable of learning long-term dependencies. In addition to the hidden state (h), which is common to all RNNs, an LSTM memory block is composed of a cell state (C), an input gate (i), an output gate (o), and a forget gate (f). The cell state is responsible for remembering information over arbitrary time intervals. The gates are made up of a sigmoid activation function (σ) and a pointwise multiplication operation ($\otimes$). Intuitively, each of the three gates can be thought of as a regulator of the information that is contained in the cell state.

Given an input sequence m_k, $k = 1, ..., T$, where T is the length of the input sequence, the LSTM evaluates the mapping of the inputs to the predicted output sequence y_k by looping through the following equations:

$$i_k = \sigma(w_i m_k + U_i h_{k-1} + b_i) \tag{3}$$

$$f_k = \sigma\left(w_f m_k + U_f h_{k-1} + b_f\right) \tag{4}$$

$$o_k = \sigma(w_o m_k + U_o h_{k-1} + b_o) \tag{5}$$

$$\widetilde{C}_k = \tanh(w_c m_k + U_c h_{k-1} + b_c) \tag{6}$$

$$C_k = f_k \otimes C_{k-1} + i_k \otimes \widetilde{C}_k \tag{7}$$

$$h_k = o_k \otimes \tanh(C_k) \tag{8}$$

$$y_k = w_y h_k + b_y \tag{9}$$

where w_i, w_f, and w_o are the weights for the input, forget, and output gates to the input, respectively. U_i, U_f, and U_o are the matrices of the weights from the input, forget, and output gates to the hidden states, respectively. b_i, b_f, and b_o are the bias vectors associated with the input, forget, and output gates. The predicted output from the

LSTM is calculated using Equation (9), where w_y and b_y denote the weight matrix and bias vector for the output, respectively.

3 | METHODOLOGY

3.1 | Development of the LSTM model

In this section, we discuss the development of an LSTM model for an agro-hydrological system using training data obtained from the Richards equation. Particularly, the model development includes the generation of the dataset, a specification of the model's framework, and the training process.

3.1.1 | Data generation

In this work, we focus on infiltration processes in agro-hydrological systems. Infiltration is often assumed to be a 1D process in the vertical direction[27]; thus, the 1D Richards equation in the z-direction is used in this work. Furthermore, the 1D Richards equation is suitable for homogeneous soils in which vertical flow is dominant, and it can also be invoked at multiple locations in heterogeneous soils. The 1D Richards equation is expressed as:

$$c(\psi)\frac{\partial \psi}{\partial t} = \frac{\partial}{\partial z}\left[K(\psi)\left(\frac{\partial \psi}{\partial z}+1\right)\right] - \rho(\psi)\mathcal{R}\left(K^c, ET^0, z_r\right). \tag{10}$$

Remark 1. The 1D Richards equation that is adopted in this work is unable to account for horizontal variability in soils. Thus, in instances where there exists significant geospatial variation in the field under examination, higher dimensional versions of the Richards equation will be more suitable.

Equation (10) is solved numerically using the method of lines approach. The central difference scheme is used to approximate the spatial derivative. The numerical solution of the Richards equation under some soil conditions, particularly extremely dry and wet conditions, is known to be unreliable.[27] To this end, several steps are adopted in the numerical scheme to guarantee reliable numerical results under such conditions. To ensure solution convergence under wet conditions, three measures are employed in this work. First, to prevent the capillary capacity from assuming a value of 0 under wet conditions, a specific storage coefficient of the soil medium is included in the parametrized equation of $c(\psi)$. Second, the numerical scheme is adapted such that only multiplication with $c(\psi)$ occurs to eliminate a degenerate solution when $c(\psi)$ assumes arbitrarily small values. Third, an implicit scheme, specifically the backward differentiation formula, is used to approximate the temporal derivative to ensure convergence. To handle unreliable solutions under dry conditions, very high reference ET^0 values are avoided during the simulation of the Richards equation. The final representation of the 1D Richards equation, after carrying out the temporal and spatial discretizations, is expressed as:

$$\begin{aligned} c_k^{p+1}(\psi)\left(\frac{\psi_k^{p+1}-\psi_k^p}{\Delta t}\right) = \Bigg(\frac{1}{\Delta z_k}\Bigg[K^p_{k+\frac{1}{2}}(\psi)\left(\frac{\psi_{k+1}^{p+1}-\psi_k^{p+1}}{\Delta z_N}+1\right) \\ - K^p_{k-\frac{1}{2}}(\psi)\left(\frac{\psi_k^{p+1}-\psi_{k-1}^{p+1}}{\Delta z_S}+1\right)\Bigg]\Bigg) \\ - \rho(\psi)\mathcal{R}_k(\cdot) \end{aligned} \tag{11}$$

where $k \in [1, N_z]$ and N_z is the number of nodes in the z-direction. $\Delta z_N = z_{k+1} - z_k$, $\Delta z_S = z_k - z_{k-1}$, $\Delta z_k = \frac{1}{2}(z_{k+1} - z_{k-1})$, and $K_{k\pm\frac{1}{2}}(\psi) \approx \frac{1}{2}(K(\psi_k) + K(\psi_{k\pm1}))$. p and Δt represent the time level and time step, respectively. The depth dependent root water uptake model, Equation (12), proposed by Feddes et al.,[28] is used as the sink term in this work.

$$\mathcal{R}_k\left(K^c, ET^0, z_r\right) = \frac{2K^c ET^0}{z_r}\left(1 - \frac{k\Delta z_k}{z_r}\right) \tag{12}$$

Equation (11) is solved numerically for the following initial and boundary conditions:

$$\psi_k(t=0) = \psi^{\text{init}} \tag{13}$$

$$\left.\frac{\partial(\psi+z)}{\partial z}\right|_{z=H_z} = 1 \tag{14}$$

$$\left.\frac{\partial \psi}{\partial z}\right|_{z=0} = -1 - \frac{u^{\text{irrig}}}{K(\psi)} \tag{15}$$

H_z and u^{irrig} [LT^{-1}] in Equations (14) and (15) represent the depth of the soil column and the irrigation rate, respectively. Equation (11), together with the initial

and boundary conditions, is expressed in state space form as:

$$x_{k+1} = F(x_k, u_k) + \omega_k \tag{16}$$

where $x_k \in \mathbb{R}^{N_x}$ represents the state vector containing $N_x = N_z$ capillary pressure head values for the corresponding spatial nodes. u_k represents the input vector containing the irrigation rate, precipitation, daily reference evapotranspiration, and the crop coefficient. ω_k is the model disturbance.

Extensive open-loop simulations are conducted to generate a dataset that captures the soil water content dynamics. Using randomly generated initial states x_0, Equation (16) is solved for randomly generated inputs to obtain a large number of state trajectories. To ensure a small temporal truncation error, the open-loop simulations are performed with a small time step size. Some level of noise is included in the open-loop simulations to account for model uncertainty. In this work, model uncertainty is due to the numerical approximation that is used to solve the Richards equation and imprecise knowledge of the empirical soil hydraulic parameters. The inclusion of noise in the data generation step can also improve the generalization ability and the robustness of the LSTM. Finally, the time-series data obtained from the open-loop simulations are partitioned into training, validation, and test datasets.

Remark 2. To accurately describe the dynamics of water in a given soil, the Richards equation requires accurate knowledge of the empirical soil hydraulic parameters. In an instance where these parameters are not known, soil moisture observations from the field, together with parameter estimation techniques, can be employed to estimate these parameters.

3.1.2 | Proposed LSTM model and model training

For irrigation scheduling purposes, it suffices to focus on the soil moisture dynamics in the root zone of the investigated soil column. Thus, we propose an LSTM model that predicts the root zone capillary pressure head in an agro-hydrological system. Specifically, the LSTM is trained to predict the one-day-ahead root zone capillary pressure head x_{t+1} using the present and the past root zone capillary pressure head inputs $x(t = 0, ..., l)$, the present and past irrigation rate inputs $u^{\text{irrig}}(t = 0, ..., l)$, the present and past rain inputs $r(t = 0, ..., l)$, the present and past crop coefficient inputs $K^c(t = 0, ..., l)$, and the present and past reference evapotranspiration inputs $ET^0(t = 0, ..., l)$. l is the time lag used for the model development, whose value is determined through experimentation. The proposed LSTM model can thus be described as a multiple input and single output system. To realize the LSTM model, the states outside the root zone are discarded from the datasets and the resulting datasets are resampled to a time frame of 1 day. In addition to approximating the complex 1D Richards equation, the proposed LSTM model can also be thought of as a reduced model since it has fewer states (lower order) compared to Equation (16).

Before training the LSTM model, the datasets are normalized to rescale the input and output variables. The LSTM model is trained with the Keras Deep Learning Library in Python. The optimal number of layers and LSTM units is determined through experimentation. During the training process, an optimization problem that minimizes the modelling error is solved using an adaptive moment estimation algorithm (i.e., Adam in Keras). The mean squared error between the predicted states and the actual states in the training dataset is chosen as the loss function for the optimization problem. To prevent over-fitting of the LSTM model, the training process is terminated when the error in the validation stops decreasing.

Remark 3. Though the proposed LSTM model is identified with simulated data from the Richards equation, it can also be developed with field data obtained from soil moisture and climate monitoring networks. After applying some data cleaning and preprocessing steps to the field data, the steps outlined in Section 3.1.2 can be applied to the resulting dataset straightforwardly.

3.2 | Scheduler design–mixed-integer MPC

The proposed scheduler (Figure 2) is designed in the mixed-integer MPC with zone control framework. The scheduler considers a prediction horizon of up to a few weeks, and its objective is to ensure optimal water uptake in crops while minimizing total water consumption and irrigation cost (e.g., pumping, electricity, maintenance costs, etc.). In this design, the scheduler ensures optimal water uptake in crops by maintaining the root zone capillary pressure head within a target zone. Using past weather data, the daily weather forecast, the root zone capillary pressure head measurement, and the identified

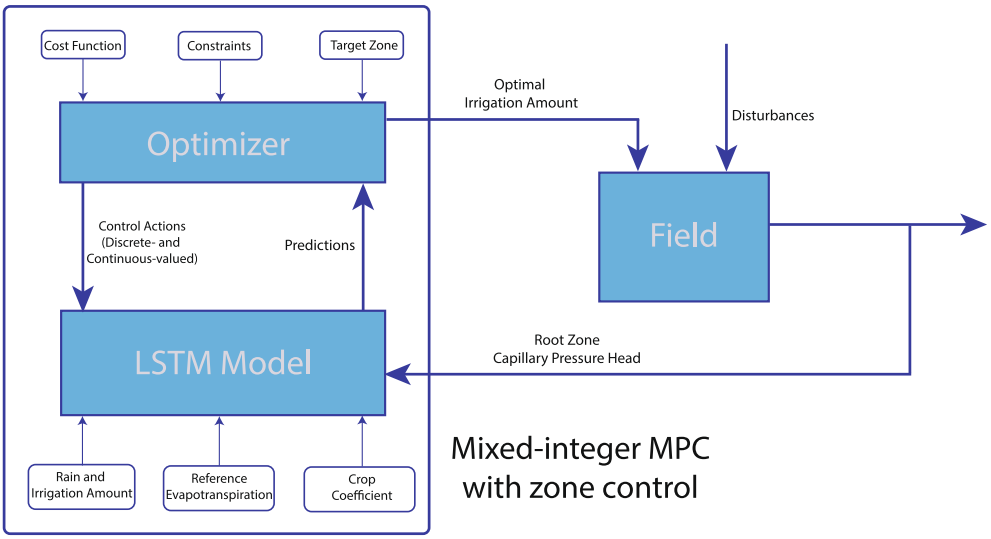

FIGURE 2 A block diagram of the proposed irrigation scheduler. LSTM, long short-term memory; MPC, model predictive control

LSTM model, the scheduler prescribes the daily discrete irrigation decision and the daily irrigation rate that achieves its objective. The soft constraint approach is used to realize zone control in this design. In this approach, slack variables are introduced in the formulation to relax the bounds of the target zone. At the same time, the slack variables are included in the objective function. For a fixed prediction/planning horizon of N days, the scheduler $\mathbb{P}_{\text{MINLP}}(y)$ is formulated as follows:

$$\min_{\boldsymbol{y},\overline{\epsilon},\underline{\epsilon},\boldsymbol{u}^{\text{irrig}},\boldsymbol{c}} \sum_{k=1}^{N}\left[\overline{Q}\overline{\epsilon}_k^2+\underline{Q}\underline{\epsilon}_k^2\right]+\sum_{k=0}^{N-1}R_c c_k+\sum_{k=0}^{N-1}R_u u_k^{\text{irrig}} \quad (17a)$$

s.t.

$$y_{k+1}=\mathcal{F}\left(\{y\}_{k-l}^{k},\{K^c\}_{k-l}^{k},\{ET^0\}_{k-l}^{k},\{u^{\text{irrig}}\}_{k-l}^{k},\eta\right), \quad k\in[0,N-1] \quad (17b)$$

$$y_0=y(0) \quad (17c)$$

$$\underline{\nu}-\underline{\epsilon}_k\le y_k\le\overline{\nu}+\overline{\epsilon}_k, \quad k\in[1,N] \quad (17d)$$

$$c_k\underline{u}^{\text{irrig}}\le u_k^{\text{irrig}}\le c_k\overline{u}^{\text{irrig}}, \quad k\in[0,N-1] \quad (17e)$$

$$c_k=\{0,1\}, \quad k\in[0,N-1] \quad (17f)$$

$$\underline{\epsilon}_k\ge 0,\quad \overline{\epsilon}_k\ge 0, \quad k\in[1,N] \quad (17g)$$

where $k\in\mathbb{Z}^+$, $\boldsymbol{y}:=[y_0,\ y_1,\ ...,\ y_N]$, $\overline{\epsilon}:=[\overline{\epsilon}_1,\overline{\epsilon}_2,...,\overline{\epsilon}_N]$, $\underline{\epsilon}:=[\underline{\epsilon}_1,\underline{\epsilon}_2,...,\underline{\epsilon}_N]$, $\boldsymbol{c}:=[c_0,\ c_1,\ ...,\ c_{N-1}]$, $\boldsymbol{u}^{\text{irrig}}:=\left[u_0^{\text{irrig}},u_1^{\text{irrig}},...,u_{N-1}^{\text{irrig}}\right]$, and $\{\gamma\}_{k-l}^{k}:=[\gamma_{k-l},\gamma_{k-l-1},\gamma_{k-l-2},..,\gamma_k]$ where $\gamma\in[y,K^c,ET^0,u^{\text{irrig}}]$. $\underline{\epsilon}_k$ and $\overline{\epsilon}_k$ (17a, 17g) are non-negative slack variables that are introduced to relax the target capillary pressure head range/zone $(\underline{\nu}_k,\overline{\nu}_k)$ in (17d). $\underline{Q}$ and $\overline{Q}$ are the per-unit costs associated with the violation of the lower and upper bounds of the target zone, respectively. R_c is the fixed cost associated with the operation of the irrigation implementing system, and R_u is the per-unit cost of the irrigation rate u^{irrig}. The binary variable (c) encodes the daily discrete irrigation decision. The cost function (17a) incorporates the objectives of maintaining the root zone capillary pressure head in a target zone in order to ensure optimal water uptake in crops by minimizing the violation of the target zone $\sum_{k=1}^{N}\left[\overline{Q}\overline{\epsilon}_k^2+\underline{Q}\underline{\epsilon}_k^2\right]$, minimizing the irrigation cost $\sum_{k=0}^{N-1}R_c c_k$, and minimizing the irrigation amount $\sum_{k=0}^{N-1}R_u u_k^{\text{irrig}}$. Constraint (17b) corresponds to the LSTM model of the root zone capillary pressure head, and η in this constraint represents the weights and bias terms associated with the identified LSTM model. In this work, the initial state is assumed to be measured and it is represented with Constraint (17c). In instances where it is not available for measurement, state estimation techniques can be employed to estimate it. See the work of Bo et al.[23] for state estimation in agro-hydrological systems. Constraint (17e) is the amount of water that can be supplied during the irrigation event on day k. When the irrigation decision on day k is a 'no decision' ($c_k = 0$), Constraint (17e) specifies that the irrigation rate must necessarily be 0. On the other hand, when the irrigation decision on a particular day is a 'yes decision' ($c_k = 1$), this constraint states that the prescribed irrigation rate must be at least equal to its lower bound ($\underline{u}^{\text{irrig}}$) and must be no larger than its upper bound ($\overline{u}^{\text{irrig}}$).

There are, at least, two main benefits associated with the inclusion of a binary variable in the proposed scheduler. First, the binary variable permits a direct inclusion of the fixed cost associated with the

operation of the irrigation implementing equipment in the objective function. With this, decisions about the cost of operating the irrigation implementing equipment can be made while guaranteeing optimal plant development. Second, the binary variable discourages the scheduler from prescribing very small irrigation amounts frequently since every nonzero irrigation rate will incur an additional cost, which is the cost associated with the operation of the irrigation implementing equipment. Thus, there is a higher incentive to prescribe relatively larger irrigation rates in a single irrigation event to minimize the cost of operating the irrigation equipment.

The solution to the optimization problem $\mathbb{P}_{\text{MINLP}}(y)$ is a sequence of predicted states $\boldsymbol{y}$, optimal slack variables ($\overline{\epsilon}$, $\underline{\epsilon}$), optimal irrigation decisions ($\boldsymbol{c}$), and optimal irrigation amounts ($\boldsymbol{u}$).

3.3 | Scheduler design–sigmoid approximation

It is desirable to develop modifications to mixed-integer problems to ensure that they can be executed in real-time. This is necessary because mixed-integer programming belongs to the class of $\mathcal{NP}-$ complete problems and, thus, can require extensive computation time and resources for problems with many integer variables. To this end, a heuristic method that approximates the binary variable in the mixed-integer formulation, which was originally applied to transmission expansion problems[29] and active power losses minimization problems,[30] is employed. Specifically, the binary variable in $\mathbb{P}_{\text{MINLP}}(y)$ is replaced with a sigmoid function $\omega(r)$ which is defined as:

$$\omega(r) = \frac{1}{1+e^{-\beta r}} \tag{18}$$

where β is the slope of the sigmoid function and the argument r is a real number. The inclusion of Equation (18) in $\mathbb{P}_{\text{MINLP}}(y)$ results in the following nonlinear programming problem $\mathbb{P}_{\text{SIG}}(y)$:

$$\min_{\mathbf{y},\overline{\epsilon},\underline{\epsilon},\mathbf{u}^{\text{irrig}},\mathbf{r}} \sum_{k=1}^{N}\left[\overline{Q}\overline{\epsilon}_k^2 + \underline{Q}\underline{\epsilon}_k^2\right] + \sum_{k=0}^{N-1} R_c\omega(r_k) + \sum_{k=0}^{N-1} R_u u_k^{\text{irrig}} \tag{19a}$$

s.t.

$$y_{k+1} = \mathcal{F}\left(\{y\}_{k-l}^{k}, \{K^c\}_{k-l}^{k}, \{ET^0\}_{k-l}^{k}, \{u^{\text{irrig}}\}_{k-l}^{k}, \eta\right), \quad k \in [0, N-1] \tag{19b}$$

Algorithm 1 **Algorithm for approximating $\boldsymbol{c}$ with $\omega(\boldsymbol{r})$**

Require: $y(0)$, $\boldsymbol{y}^0$, $\boldsymbol{r}^0$, $(\boldsymbol{u}^{\text{irrig}})^0$, ζ, β^0, τ
  $\boldsymbol{y}_{\text{guess}} \leftarrow \boldsymbol{y}^0$
  $\boldsymbol{r}_{\text{guess}} \leftarrow \boldsymbol{r}^0$
  $(\boldsymbol{u}^{\text{irrig}})_{\text{guess}} \leftarrow (\boldsymbol{u}^{\text{irrig}})^0$
  $\beta \leftarrow \beta^0$
  $i \leftarrow 0$
  while $\|\omega(\boldsymbol{r}^i) - \boldsymbol{c}\|_2 > \zeta$ **do**
  Solve $\mathbb{P}_{\text{SIG}}(y(0))$ for β^i
    $\boldsymbol{y}_{\text{guess}} \leftarrow \boldsymbol{y}^i$
    $\boldsymbol{r}_{\text{guess}} \leftarrow \boldsymbol{r}^i$
    $(\boldsymbol{u}^{\text{irrig}})_{\text{guess}} \leftarrow (\boldsymbol{u}^{\text{irrig}})^i$.
    $\beta^{i+1} \leftarrow \tau\beta^i$
    $i \leftarrow i+1$
  end while

$$y_0 = y(0) \tag{19c}$$

$$\underline{\nu} - \underline{\epsilon}_k \le y_k \le \overline{\nu} + \overline{\epsilon}_k, \quad k \in [1, N] \tag{19d}$$

$$\omega(r_k)\underline{u}^{\text{irrig}} \le u_k^{\text{irrig}} \le \omega(r_k)\overline{u}^{\text{irrig}}, \quad k \in [0, N-1] \tag{19e}$$

$$r_{\min} \le r_k \le r_{\max}, \quad k \in [0, N-1] \tag{19f}$$

$$\underline{\epsilon}_k \ge 0, \quad \overline{\epsilon}_k \ge 0, \quad k \in [1, N] \tag{19g}$$

where $\boldsymbol{r} := [r_0, r_1, ..., r_{N-1}]$. $\mathbb{P}_{\text{SIG}}(y)$ can thus be solved with a suitable NLP algorithm.

3.3.1 | Selection of β

The sigmoid function converges to binary elements (0 or 1) for higher values of its slope β. However, the use of very large β values often results in an ill-conditioned optimization. To handle this issue, an algorithm is proposed to improve the convergence of the sigmoid function to binary elements while reducing ill-conditioning issues. This process involves successively solving $\mathbb{P}_{\text{SIG}}(y)$ for increasing values of β (by a factor of τ in Algorithm 1) until a predetermined convergence criterion is met. This predefined criterion, for the i^{th} evaluation of $\mathbb{P}_{\text{SIG}}(y)$, can be mathematically expressed as:

$$\left\|\omega(\mathbf{r}^i) - \mathbf{c}\right\|_2 \le \zeta \tag{20}$$

where $\boldsymbol{c}$ is a vector of binary elements. Each element of $\boldsymbol{c}$ corresponds to the nearest binary value of each element of $\omega(\boldsymbol{r}^i)$. ζ represents the convergence tolerance. The detailed steps are described in Algorithm 1.

3.4 | Scheduler design for spatially variable fields

Due to the biological, chemical, and physical processes that occur in agro-hydrological systems, high spatial variability is commonly found in soils. Consequently, irrigation scheduling that assumes a uniform field (uniform water application rate) is not the most effective approach and, thus, the scheduler formulation described in Section 3.2 is not suitable for irrigation scheduling in spatially variable fields. It is necessary to characterize the within-field spatial variability during the determination of irrigation schedules to ensure improved water use efficiency and increased crop productivity. The basic approach to spatially variable irrigation scheduling is to delineate a spatially variable field into distinct irrigation management zones/areas.[31,32] Irrigation management zones are sub-field areas with homogeneous properties that are known to affect the yield of crops. A field can be delineated into irrigation management zones based on soil texture, elevation, topography, experience, and drainage, among others. The irrigation timing and the water application depth can then be optimized for each distinct management zone. Motivated by the above, it is important to adapt the proposed scheduler to irrigation scheduling in spatially variable fields. To this end, we employ the following steps:

1. The spatially variable field under consideration is divided into definite management zones. The delineation of the field into irrigation management zones may be done based on soil texture, elevation, and drainage, among others.
2. An LSTM model is then trained for each management zone using simulated data from the 1D Richards equation, according to the steps outlined in Section 3.1.
3. Irrigation can then be scheduled using the root zone capillary pressure head measurement for each irrigation management zone. It is worth noting that all areas within a given management zone receive the same irrigation amount. However, the irrigation amount may vary from one irrigation management zone to another.

In the context of spatially variable irrigation scheduling, we propose separate formulations that apply to small-scale and large-scale fields. The detailed formulations are described in the sequel.

3.4.1 | Spatially variable irrigation scheduling for small-scale fields

In this paper, a spatially variable field with distinct management zones is considered a small-scale field if the irrigation implementing equipment can irrigate all the management zones in 1 day. For such fields, in principle, the irrigation implementing equipment can irrigate all the management zones each day within the prediction horizon. Irrigation scheduling in small-scale spatially variable fields should thus reflect this observation to avoid over/under irrigation. For M irrigation management zones, the scheduler for a small-scale spatially variable field $\mathbb{P}_{\text{SV-SS}}(y)$ can be formulated as follows:

$$\min_{\mathbf{Y},\overline{\mathbf{E}},\underline{\mathbf{E}},\mathbf{U}^{\text{irrig}},\mathbf{c}} \sum_{j=1}^{M}\sum_{k=1}^{N}\left[\overline{Q}(j)\overline{\epsilon}_{jk}^2+\underline{Q}(j)\underline{\epsilon}_{jk}^2\right]+R_c\sum_{k=0}^{N-1}c_k +R_u\sum_{j=1}^{M}\sum_{k=0}^{N-1}u_{jk}^{\text{irrig}} \tag{21a}$$

s.t.

$$y_{j(k+1)}=\mathcal{F}^j\left(\left\{y_j\right\}_{k-l}^{k},\left\{K_j^c\right\}_{k-l}^{k},\left\{ET^0\right\}_{k-l}^{k},\left\{u_j^{\text{irrig}}\right\}_{k-l}^{k},\eta_j\right), \quad j\in\widetilde{M},k\in[0,N-1] \tag{21b}$$

$$y_{j0}=y_j(0), \qquad j\in\widetilde{M} \tag{21c}$$

$$\underline{\nu}_j-\underline{\epsilon}_{jk}\le y_{jk}\le\overline{\nu}_j+\overline{\epsilon}_{jk}, \qquad j\in\widetilde{M},k\in[1,N] \tag{21d}$$

$$c_k\underline{u}_j^{\text{irrig}}\le u_{jk}\le c_k\overline{u}_j^{\text{irrig}}, \qquad j\in\widetilde{M},k\in[0,N-1] \tag{21e}$$

$$c_k\in\{0,1\}, \qquad k\in[0,N-1] \tag{21f}$$

$$\underline{\epsilon}_{jk}\ge 0,\quad \overline{\epsilon}_{jk}\ge 0, \qquad j\in\widetilde{M},k\in[1,N] \tag{21g}$$

where $j\in\mathbb{Z}^+$, $k\in\mathbb{Z}^+$, $\boldsymbol{Y}:=[\boldsymbol{y}_1,\boldsymbol{y}_2,\ldots,\boldsymbol{y}_M]$, $\overline{\mathbf{E}}:=[\overline{\epsilon}_1,\overline{\epsilon}_2,\ldots,\overline{\epsilon}_M]$, $\underline{\mathbf{E}}:=[\underline{\epsilon}_1,\underline{\epsilon}_2,\ldots,\underline{\epsilon}_M]$, and $\mathbf{U}^{\text{irrig}}:=\left[\mathbf{u}_1^{\text{irrig}},\mathbf{u}_2^{\text{irrig}},\ldots,\mathbf{u}_M^{\text{irrig}}\right]$. $\widetilde{M}$ is a closed set that contains the $[j_1,j_2,\ldots,j_M]$ positional indices of the M management zones.

In essence, formulation $\mathbb{P}_{\text{SV-SS}}(y)$ seeks to replicate formulation $\mathbb{P}_{\text{MINLP}}(y)$ for all the M irrigation management zones under consideration. However, in all the management zones, the binary variables that are defined for the planning horizon are the same. This is done to realize a uniform daily irrigation decision in all the irrigation management zones. A uniform daily irrigation

decision in all the management zones satisfies the assumption that the irrigation implementing equipment can irrigate all the management zones in 1 day.

3.4.2 | Spatially variable irrigation scheduling for large-scale fields

In this paper, a spatially variable field with M distinct management zones is considered a large-scale field if the irrigation implementing equipment takes more than 1 day to irrigate the entire field. Specifically, we consider a scenario where the irrigation implementing equipment spends 1 day irrigating each management zone and thus spends M days irrigating the entire field. For such fields, depending on the order in which the irrigation implementing equipment irrigates the management zones during a single irrigation cycle, each management zone can be irrigated on specific days within the prediction horizon. This scenario is best illustrated with a concrete example. Assuming that the spatially variable field under consideration consists of two management zones (M_1, M_2), and also supposing that the irrigation implementing equipment starts each irrigation cycle from M_1, then for a prediction horizon of 14 days, the irrigation implementing equipment completes its irrigation cycle in 2 days and can thus be operated 7 times within the prediction horizon. Additionally, M_1 can only be irrigated on days 1, 3, 5, 7, ..., 13, while M_2 can only be irrigated on days 2, 4, 6, ..., 14. The determination of irrigation schedules for such a field should be made to reflect this arrangement to ensure optimal uptake of water by crops. Before introducing the formulation for an arbitrary number of management zones and an arbitrary prediction horizon, for the sake of simplicity and with no loss of generality, we assume that the order in which the irrigation implementing equipment irrigates the entire field coincides with the indices assigned to the M management zones. The scheduler for a large-scale spatially variable field $\mathbb{P}_{\text{SV-LS}}(y)$ can be formulated as follows:

$$\min_{\mathbf{Y},\overline{\mathbf{E}},\underline{\mathbf{E}},\mathbf{U}^{\text{irrig}},\mathbf{c}} \sum_{j=1}^{M}\sum_{k=1}^{N}\left[\overline{Q}(j)\overline{\epsilon}_{jk}^{2}+\underline{Q}(j)\underline{\epsilon}_{jk}^{2}\right]+R_c\sum_{n=1}^{N_c}c_n +R_u\sum_{j=1}^{M}\sum_{k=0}^{N-1}u_{jk}^{\text{irrig}} \tag{22a}$$

s.t.

$$y_{j(k+1)}=\mathcal{F}^{j}\left(\left\{y_j\right\}_{k-l}^{k},\left\{K_j^{c}\right\}_{k-l}^{k},\left\{ET^{0}\right\}_{k-l}^{k},\left\{u_j^{\text{irrig}}\right\}_{k-l}^{k},\eta_j\right), \quad j\in\widetilde{M},k\in[0,N-1] \tag{22b}$$

$$y_{j0}=y_j(0), \qquad j\in\widetilde{M} \tag{22c}$$

$$\underline{\nu}_j-\underline{\epsilon}_{jk}\le y_{jk}\le\overline{\nu}_j+\overline{\epsilon}_{jk}, \qquad j\in\widetilde{M},k\in[1,N] \tag{22d}$$

$$\begin{cases} c_n\underline{u}_{j_1}^{\text{irrig}}\le u_{j_1k}\le c_n\overline{u}_{j_1}^{\text{irrig}}, & n\in[1,\ N_c]\\ u_{jk}=0 & j\in\widetilde{M}\setminus j_1\end{cases},\quad B=\{Mi+j_1:i\in[0,\ N_c)\} \tag{22e}$$

$$\begin{cases} c_n\underline{u}_{j_2}^{\text{irrig}}\le u_{j_2k}\le c_n\overline{u}_{j_2}^{\text{irrig}}, & n\in[1,\ N_c]\\ u_{jk}=0 & j\in\widetilde{M}\setminus j_2\end{cases},\quad B=\{Mi+j_2:i\in[0,\ N_c)\} \tag{22f}$$

$$\vdots$$

$$\begin{cases} c_n\underline{u}_{j_M}^{\text{irrig}}\le u_{j_Mk}\le c_n\overline{u}_{j_M}^{\text{irrig}}, & n\in[1,\ N_c]\\ u_{jk}=0 & j\in\widetilde{M}\setminus j_M\end{cases},\quad B=\{Mi+j_M:i\in[0,\ N_c)\} \tag{22g}$$

$$c_n\in\{0,1\}, \qquad n\in[1,N_c] \tag{22h}$$

$$\underline{\epsilon}_{jk}\ge 0,\quad \overline{\epsilon}_{jk}\ge 0, \qquad j\in\widetilde{M},k\in[1,N] \tag{22i}$$

where $i\in\mathbb{Z}^{0+}$, $j\in\mathbb{Z}^{+}$, $k\in\mathbb{Z}^{+}$, $N_c=\frac{N}{M}$, $\widetilde{M}=[j_1,j_2,\ldots,j_M]$, and the notation $\widetilde{M}\setminus j$ refers to the closed set $\widetilde{M}$ excluding the element j. N_c represents the number of irrigation cycles that can be performed within the prediction horizon.

In this formulation, instead of defining a binary variable for each day within the prediction horizon, we define a binary variable for the N_c cycles that can be performed within N. So, for the aforementioned illustrative example, for $N=14$, $M=2$, and $\widetilde{M}=[j_1,j_2]$, N_c will have a value of $\frac{14}{2}=7$. The closed set $A=[M(n-1)+1,\ Mn]$ represents the days that make up the $n^{\text{th}}\in[1,N_c]$ cycle. Similarly, for the illustrative example, the days that make up the first cycle are days 1 and 2, the days that make up the second cycle are days 3 and 4, and so on. For the j^{th} management zone, the specific days within N on which the irrigation event can be performed is given by the sequence $B=\{Mi+j:i\in[0,\ N_c)\}$. Applying B to the illustrative example, the days on which the irrigation event can be performed in the management zone j_1 are {1, 3, 5, 7, 9, 11, 13}. For management zone j_2, the corresponding days are {2, 4, 6, 8, 10, 12, 14}. The first part of Constraints (22e–22f) determines the irrigation rate for the j^{th} management zone on all the days that make up the set B. For the n^{th} cycle, if $c_n=1$, this constraint specifies that the prescribed irrigation rate for the j^{th}

management zone must be at least equal to $\underline{u}_j^{\text{irrig}}$ and must be no larger than $\overline{u}_j^{\text{irrig}}$ on the day corresponding to $k = A \cap B$. On the other hand, if $c_n = 0$, this constraint specifies that the irrigation rate must necessarily be 0 for all the M management zones on all the k days in A. Applying this to the illustrative example means that if $c_1 = 1$, then for management zone j_1, the irrigation rate must be between $\underline{u}_{j_1}^{\text{irrig}}$ and $\overline{u}_{j_1}^{\text{irrig}}$ on day 1. Similarly, for management zone j_2, the irrigation rate must be between $\underline{u}_{j_2}^{\text{irrig}}$ and $\overline{u}_{j_2}^{\text{irrig}}$ on day 2. Additionally, if, say, $c_2 = 0$, then the irrigation rate in management zones j_1 and j_2 must be 0 on days 3 and 4, respectively. The second part of these constraints stipulates that the irrigation rate must necessarily be 0 for the remaining $\widetilde{M} \setminus j$ management zones on all the days that make up set B. This is to illustrate the fact that only one management zone can be irrigated on a particular day. Applying this to the illustrative example means that the irrigation rate for management zone j_1 must be zero on days 2, 4, 6, 8, 10, 12, and 14. Similarly, the irrigation rate must be zero on days 1, 3, 5, 7, 9, 11, and 13 for management zone j_2.

4 | SIMULATION CASE STUDIES

To evaluate the predictive capability of the proposed modelling framework, an LSTM model is first identified to predict the root zone capillary pressure head in a 0.6 m loamy-sand soil column. Before the data generation process, the soil column is spatially discretized into 30 equally spaced compartments, and each compartment is initialized with a pressure head value of −180 mm. This translates to a nodal distance of 2 cm, which is considered suitable to prevent an over- and underestimation of the infiltration and evaporation fluxes of the Richards equation. A sequence of open-loop simulations is performed for the resulting soil column with a full sweep through the irrigation amount, rain, reference evapotranspiration, and crop coefficient inputs. Specifically, to generate a dataset that adequately captures the pressure head dynamics in the investigated column, the irrigation amount, rain, daily reference evapotranspiration, and crop coefficient inputs are randomly chosen from the following respective ranges: (0.33–3.56 cm/day), (1.04–7.0 mm), (1.04–3.0 mm), and (0.50–0.88). It is worth mentioning that several open-loop simulation studies were performed to determine these input ranges. Additionally, the soil column is irrigated periodically and the time interval between any two successive irrigation events is selected at random between 2 and 6 days. Process noise is considered in the open-loop simulations and it has a zero mean with a standard deviation of 0.05 mm. Sampled data points representing the state trajectories are obtained from the open-loop simulations at a sampling time of 6 min. For this simulation experiment, the pressure head value at a depth of 0.5 m is chosen to characterize the root zone pressure head. Thus, the pressure head values at other spatial points are discarded, and the resulting noisy time series data is resampled such that the resulting dataset has a sampling time of 1 day. Fifty six thousand data points are obtained after the resampling step, and an LSTM model is subsequently developed to predict the one-day-ahead root zone capillary pressure head using the Keras API. The LSTM model is designed to have two hidden layers. Each layer consists of 200 LSTM units, and a sequence length of 5 days is used for the training. Consequently, the time lag/associated with the inputs of the LSTM model is 4. The time lag, the number of hidden layers on the network, and the number of units in each hidden layer are determined through experimentation.

In model predictive algorithms, it is required that at any given time, the process outputs be predicted many time-steps into the future. To this end, the identified LSTM model is used to predict the root zone pressure head for long periods. Particularly, these multistep-ahead predictions are produced recursively by iterating the identified one-step-ahead LSTM model, in which previously predicted pressure head values are used as inputs in successive predictions. In this paper, the mean absolute error (MAE), the root mean squared error (RMSE), and the coefficient of determination (R^2) are used to quantify the predictive capability of the identified LSTM model. The MAE and RMSE are used to quantify the prediction errors in the units of the capillary pressure head, and they are mathematically defined as:

$$MAE = \frac{1}{n}\sum_{k=1}^{n} |\, y_k - \widehat{y}_k \,| \tag{23}$$

$$RMSE = \left[\frac{\sum_{k=1}^{n}(y_k - \widehat{y}_k)^2}{n}\right]^{\frac{1}{2}} \tag{24}$$

where y_k and $\widehat{y}_k$ represent the true and predicted values of the capillary pressure head for day k. The R^2 is used to quantify the ability of the identified LSTM model to explain the variance in the observed data, and it is expressed as follows:

$$R^2 = 1 - \frac{\sum_{k=1}^{n}(y_k - \widehat{y}_k)^2}{\sum_{k=1}^{n}(y_k - \overline{y}_k)^2} \tag{25}$$

where $\overline{y}_k$ represents the mean of the true capillary pressure head values.

Three simulation case studies, namely, Case Studies 1, 2, and 3, are employed to demonstrate the utility of the scheduler designs $\mathbb{P}_{\text{MINLP}}(y)$, $\mathbb{P}_{\text{SV-SS}}(y)$, and $\mathbb{P}_{\text{SV-LS}}(y)$, respectively. Case Study 1 is based on a uniform field composed of loamy soil. The lower and upper bounds of the target zone are chosen as −820 and −690 mm, and the per unit costs associated with the violation of these zones are chosen as $\overline{Q} = \underline{Q} = 9000$. The fixed cost associated with the irrigation implementing equipment is selected as $R_c = 50$ and the per unit cost of the irrigation amount is $R_u = 20$. Two scenarios are investigated in Case Study 1: (i) Scenario 1: Absence of rain in the weather data; and (ii) Scenario 2: Presence of rain in the weather data.

The formulation $\mathbb{P}_{\text{SIG}}(y)$ is evaluated under Scenario 1 of Case Study 1 where the ability of the heuristic method to improve the computational efficiency of the proposed scheduling approach is demonstrated.

In Case Study 2, the utility of $\mathbb{P}_{\text{SV-SS}}(y)$ is evaluated for a small-scale field which is delineated into three management zones (MZs). The delineation of the field is done according to soil texture, which gives rise to a loam MZ, a loamy sand MZ, and a sand MZ. The lower and upper bounds of the target pressure head range/zone are chosen as −850 and −690 mm for the loamy soil MZ, −340 and −180 mm for the loamy sandy soil MZ, and −290 and −160 mm for the sandy soil MZ.

In Case Study 3, the utility of $\mathbb{P}_{\text{SV-LS}}(y)$ is evaluated for a large-scale field which is delineated into two management zones (MZs). The delineation of the field in this simulation experiment is also done according to soil texture, which gives rise to a loam MZ and a loamy sand MZ.

In Case Studies 2 and 3, the sigmoid function approximation versions of $\mathbb{P}_{\text{SV-SS}}(y)$ and $\mathbb{P}_{\text{SV-LS}}(y)$ are utilized, respectively. In these case studies, the values of $\overline{Q}$ and $\underline{Q}$, which are used in Case Study 1, are adopted for the loam MZ. For the loamy sand and sand MZs, $\overline{Q}$ and $\underline{Q}$ are chosen as 2000 and 9000, respectively. As in Case Study 1, the values of R_c and R_u are respectively chosen as 50 and 20 in these case studies.

A prediction horizon of 14 days is used in all the simulations, and the daily reference evapotranspiration data for the simulation period in all three case studies is depicted in Figure 3A. The rain information that is used in Scenario 2 of Case Study 1 is depicted in Figure 3B. A crop coefficient value of 0.5 is used in all the case studies. During the data generation step, for the various soil types considered in this work, the soil hydraulic parameters of the parametrized models of $K(\psi)$ and $c(\psi)$ are depicted in Table 1. This study assumed accurate knowledge of the soil hydraulic parameters, however, it is mostly the case that these parameters are known to a limited degree. In such instances, soil moisture observations from the field under consideration can be used in conjunction with a suitable parameter estimator to estimate these hydraulic parameters. See the works of Bo et al. and Bo and Liu[23,34] for a thorough study of hydraulic parameter estimation in agro-hydrological systems. In all the case studies, the scheduler is evaluated for initial states of −754 mm in the loam MZ, −279 mm in the loamy sand MZ, and −262 mm in the sand MZ. Similarly, in all the case studies, past root zone capillary pressure head values of (−795, −748, −735, and −740 mm), (−173, −212, −239, and −260 mm), and (−225, −239, −251, and −258 mm) are used in the loam, loamy sand, and sand MZs, respectively. The lower and upper bounds of the target zone in all three MZs lie below the field capacity and above the permanent wilting points of loam, loamy sand, and sandy soils. The mixed-integer and nonlinear programs arising from all the case studies are solved with the BONMIN and IPOPT solvers, respectively.

5 | RESULTS AND DISCUSSION

5.1 | Predictive capability of the LSTM model

In Figure 4A, the one-day-ahead predictions obtained from the LSTM model are compared with the actual pressure head values in the test dataset. From this figure, it is evident that the identified LSTM model can accurately model the root zone pressure head in the loamy sand soil column while capturing its general trend. In Figure 4B, the multistep-ahead predictions obtained from the identified model are compared with the actual pressure head values. From this figure, it can be seen that a recursive use of the identified LSTM model produces accurate pressure head predictions and the predictive performance is comparable to that of the 1D Richards equation. Notwithstanding the accurate predictions obtained in the multistep-ahead application, the accumulation and propagation of prediction errors in this recursive implementation results in a slight drop in the prediction performance compared to the one-step-ahead prediction.

The performance evaluation metrics for the identified LSTM model, in the one-day-ahead and multistep-ahead prediction settings are summarized in Table 2. From this table, the numerical values of the MAE and RMSE obtained in both prediction settings indicate that the identified LSTM model is able to provide good predictions. It can also be concluded from Table 2 that the identified LSTM model is able to adequately explain the

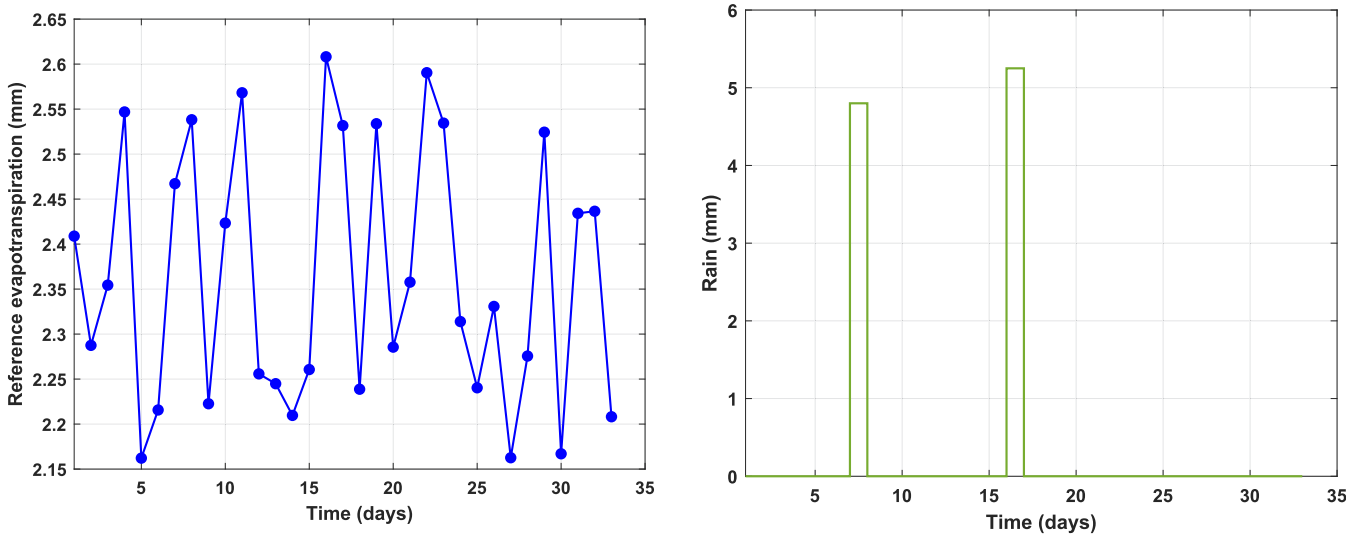

(A) Reference evapotranspiration (B) Rain forecast

FIGURE 3 Weather data for the simulation case studies

Soil type	K_s (m/s)	θ_s (m^3/m^3)	θ_r (m^3/m^3)	α (1/m)	n (–)
Loam	2.889×10^{-6}	0.430	0.078	3.600	1.56
Loamy sand	4.053×10^{-5}	0.410	0.057	12.40	2.28
Sand	8.250×10^{-5}	0.430	0.045	14.50	2.68

TABLE 1 The hydraulic parameters of soil types considered in the simulation case studies[33]

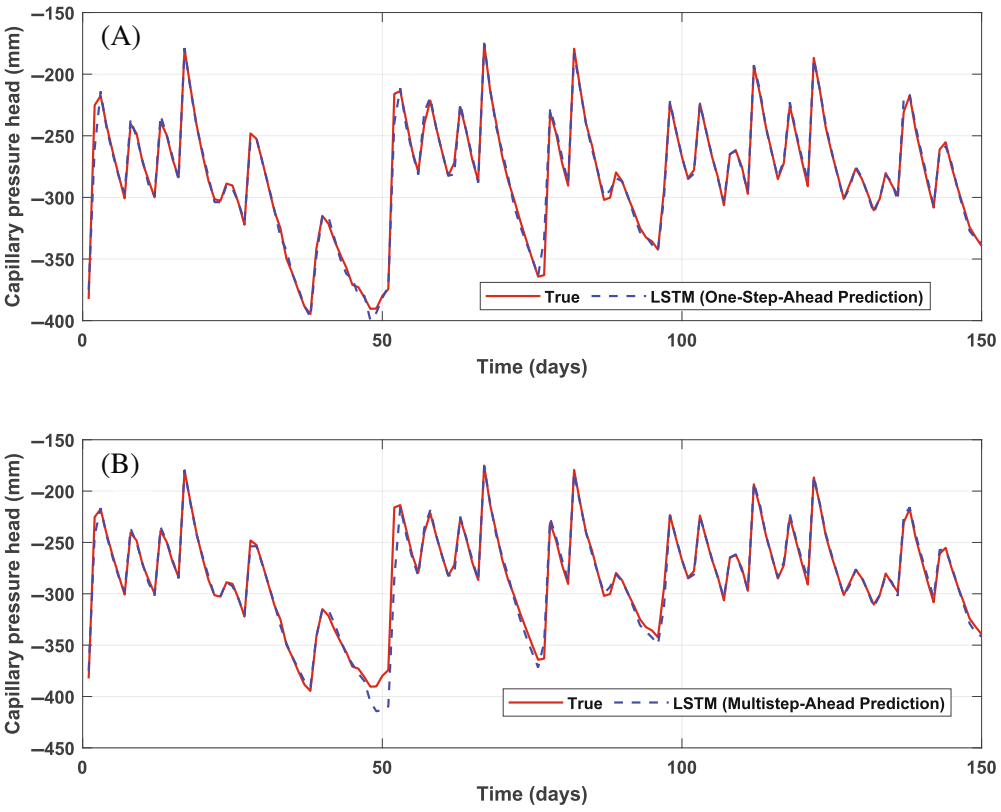

FIGURE 4 Actual root zone pressure head (red solid line) and the predicted root zone pressure head (blue dash-dot) using the test dataset, (A) one-day-ahead prediction, and (B) multistep-ahead prediction. LSTM, long short-term memory

variability in the testing data since the R^2 values obtained in both prediction settings are close to 1.

5.2 | Irrigation scheduling in homogeneous fields–Case Study 1

5.2.1 | Scenario 1

First, the results of a single evaluation (open-loop simulation) of the scheduler are analyzed. Figure 5A show the predicted state trajectory under the optimal input trajectory in Figure 5B. It can be seen that by prescribing irrigation rates of 1.25 and 1.10 cm/day on days 3 and 7, respectively, the irrigation scheduler can maintain the root zone pressure head in the target zone. Applying the open-loop predicted input sequence to the field will usually result in a deviation between the predicted root zone pressure head and the actual dynamics of the root zone pressure head. This deviation will be due to a possible mismatch between the actual field and the identified LSTM model, and additive disturbances arising from errors in weather forecast data. To this end, we consider a closed-loop implementation of the scheduler known as the receding horizon control (RHC) scheme, which is known to provide some degree of inherent robustness to these uncertainties. In this framework, only the first control input of the optimal control sequence is applied to the actual field. In this scenario, a discretized Richards equation of a 0.60 m loamy soil column is used as the actual field. To incorporate feedback into the scheduling scheme, $\mathbb{P}_{\text{MINLP}}(y)$ is evaluated at the next time instant where the current state is chosen as the pressure head value at a depth of 0.50 m in the 0.6 m loamy soil column. For this closed-loop implementation, 20 evaluations of $\mathbb{P}_{\text{MINLP}}(y)$ are performed and the simulation results are summarized in Figure 6A,B. In the closed-loop operation of the scheduler, it prescribes irrigation rates of 1.30, 1.20, 1.22, and 1.21 cm/day on days 3, 8, 15, and 20, to maintain the root zone pressure head in the target zone.

TABLE 2 Predictive performance of the identified long short-term memory model when evaluated on the test dataset for a period of 150 days

Prediction setting	MAE (mm)	RMSE (mm)	R^2 (–)
One-day-ahead	2.99	5.30	0.99
Multistep-ahead	3.88	8.31	0.97

Abbreviations: MAE, mean absolute error; RMSE, root mean squared error.

5.2.2 | Scenario 2

In this scenario, precipitation values of 4.8 and 5.2 mm are considered on days 6 and 16 of the simulation period. It can be seen from the open-loop (Figure 7A,B) and closed-loop (Figure 8A,B) trajectories that the proposed scheduler further optimized the irrigation rate by maximizing the use of the forecasted rainfall amounts. Thus, as a result of the anticipated rain on the 6th day, the open-loop implementation of the scheduler prescribes an irrigation rate of 1.25 cm/day on the 6th day (Figure 7B) and this together with the rain forecast is able to keep the root zone pressure head in the target zone (Figure 7A). Similarly, due to the anticipated rain on days 6 and 16, the closed-loop implementation of the scheduler

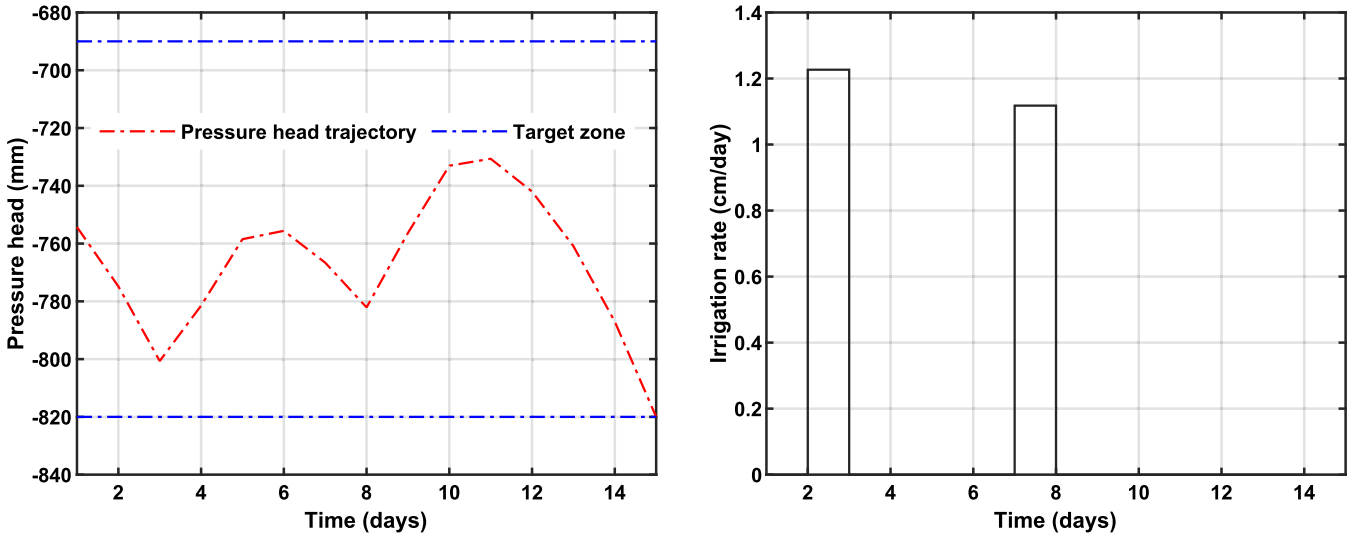

(A) Capillary pressure head. (B) Prescribed irrigation rate.

FIGURE 5 Open-loop trajectories computed by the scheduler of Equations (17a)–(17g) in Scenario 1

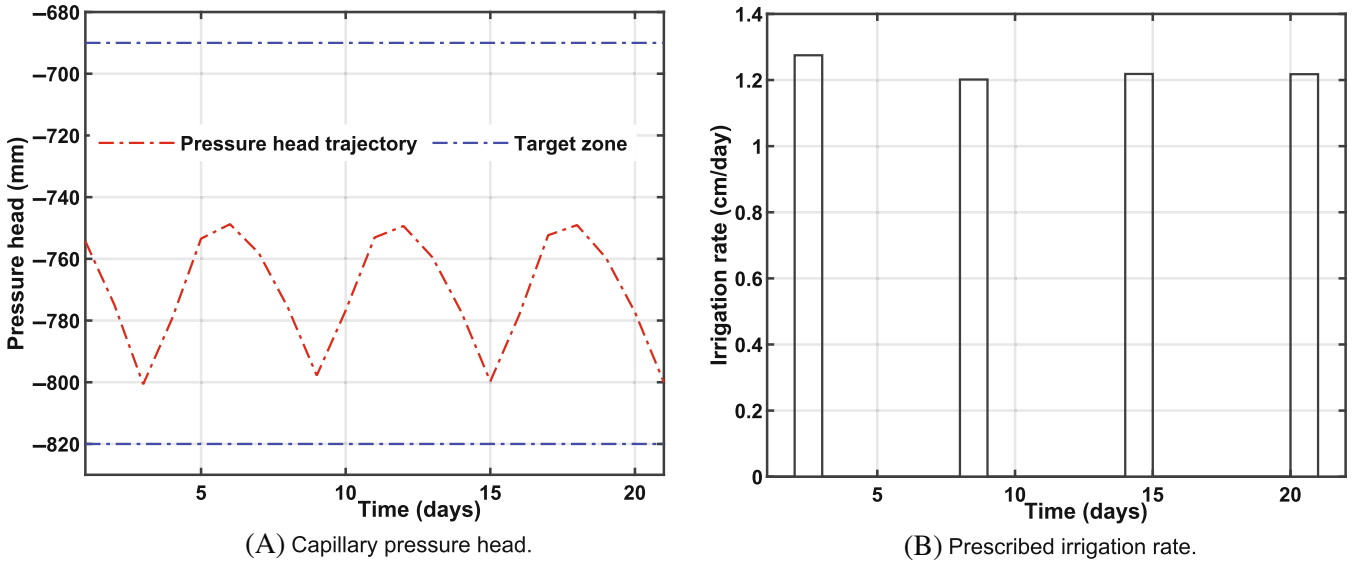

(A) Capillary pressure head. (B) Prescribed irrigation rate.

FIGURE 6 Closed-loop trajectories under the scheduler of Equations (17a)–(17g) in Scenario 1

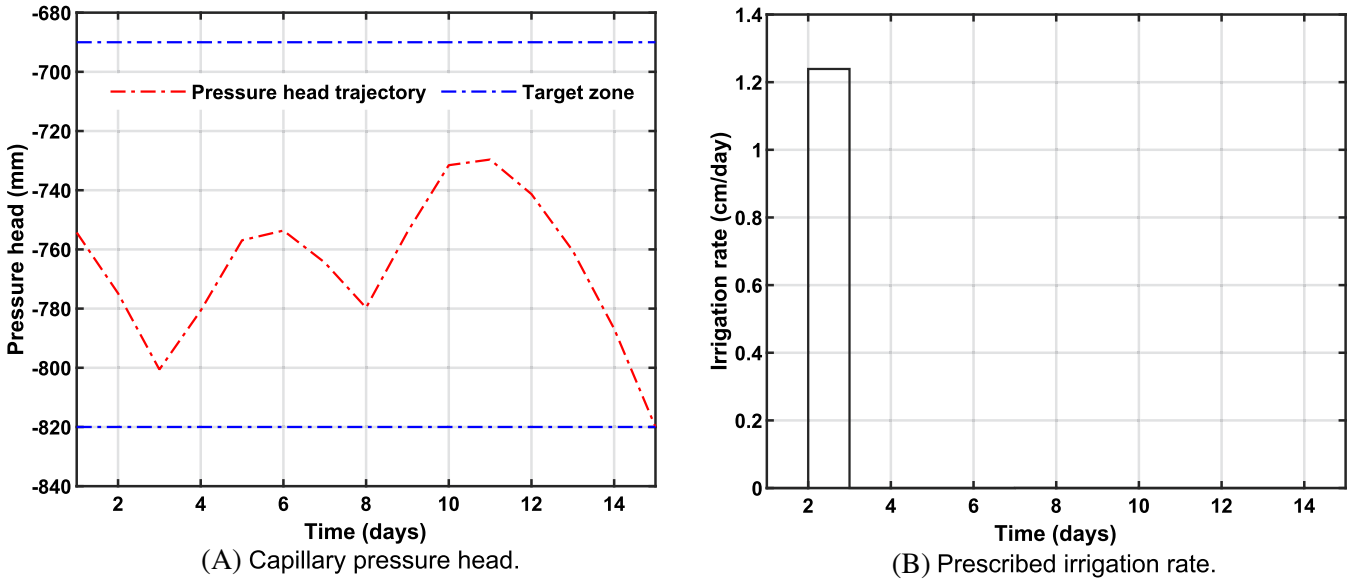

(A) Capillary pressure head. (B) Prescribed irrigation rate.

FIGURE 7 Open-loop trajectories computed by the scheduler of Equations (17a)–(17g) in Scenario 2

prescribes 1.18 cm/day and 0.7 cm/day of irrigation on days 3 and 13 (Figure 8B) to maintain the root zone pressure head in the target zone (Figure 8A).

5.3 | Performance of the heuristic method

In this section, the performance of $\mathbb{P}_{\text{SIG}}(y)$ is investigated under Scenario 1 of Case Study 1. This simulation study revealed that a slope of 25 was able to provide a good convergence of the sigmoid function to the binary elements while preventing ill-conditioning issues. This value is not expected to be suitable for all evaluations of $\mathbb{P}_{\text{SIG}}(y)$ and Algorithm 1 should be invoked in instances where it provides unsatisfactory results. From the open-loop trajectories, a visual inspection of Figure 9A,B reveal that, with a suitable slope, the heuristic method $\mathbb{P}_{\text{SIG}}(y)$ can provide the same results as the mixed-integer formulation $\mathbb{P}_{\text{MINLP}}(y)$. The values of the total cost shown in Table 3 further confirm that the open-loop trajectories computed in both formulations are one and the same. It should be noted in instances where the sigmoid function is unable to approximate the binary elements correctly, the numerical value of $\sum_{k=0}^{N-1} R_c \omega(r_k) + \sum_{k=0}^{N-1} R_u u_k^{\text{irrig}}$ in the cost function of $\mathbb{P}_{\text{SIG}}(y)$ may be smaller than that of $\sum_{k=0}^{N-1} R_c c_k + \sum_{k=0}^{N-1} R_u u_k^{\text{irrig}}$ in $\mathbb{P}_{\text{MINLP}}(y)$. This will result in a smaller overall cost for formulation $\mathbb{P}_{\text{SIG}}(y)$

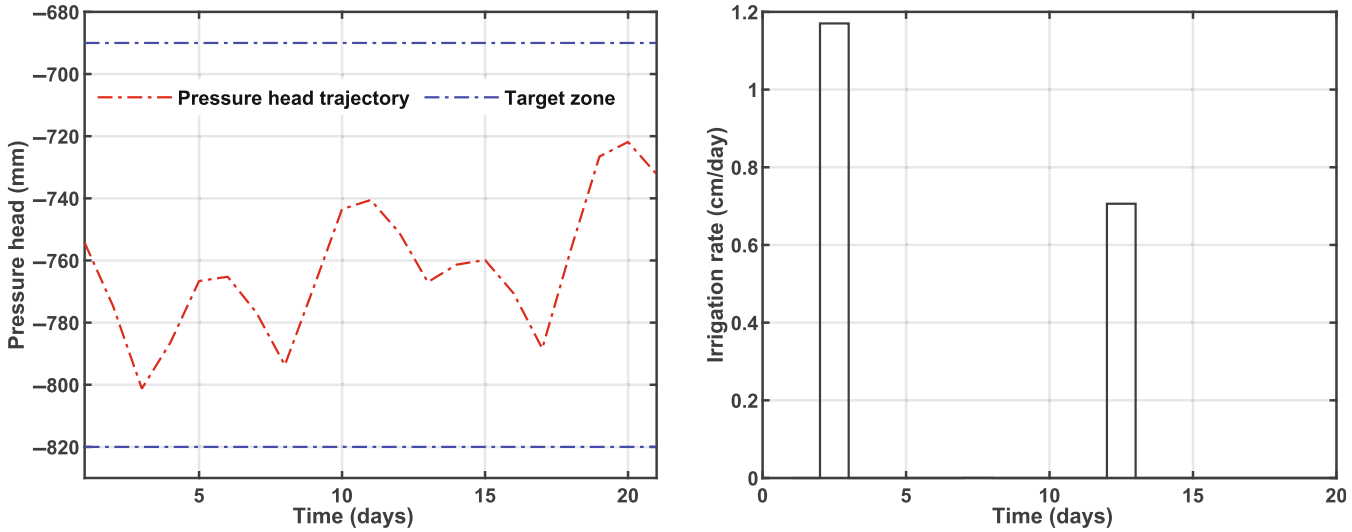

(A) Capillary pressure head. (B) Prescribed irrigation rate.

FIGURE 8 Closed-loop trajectories under the scheduler of Equations (17a)–(17g) in Scenario 2

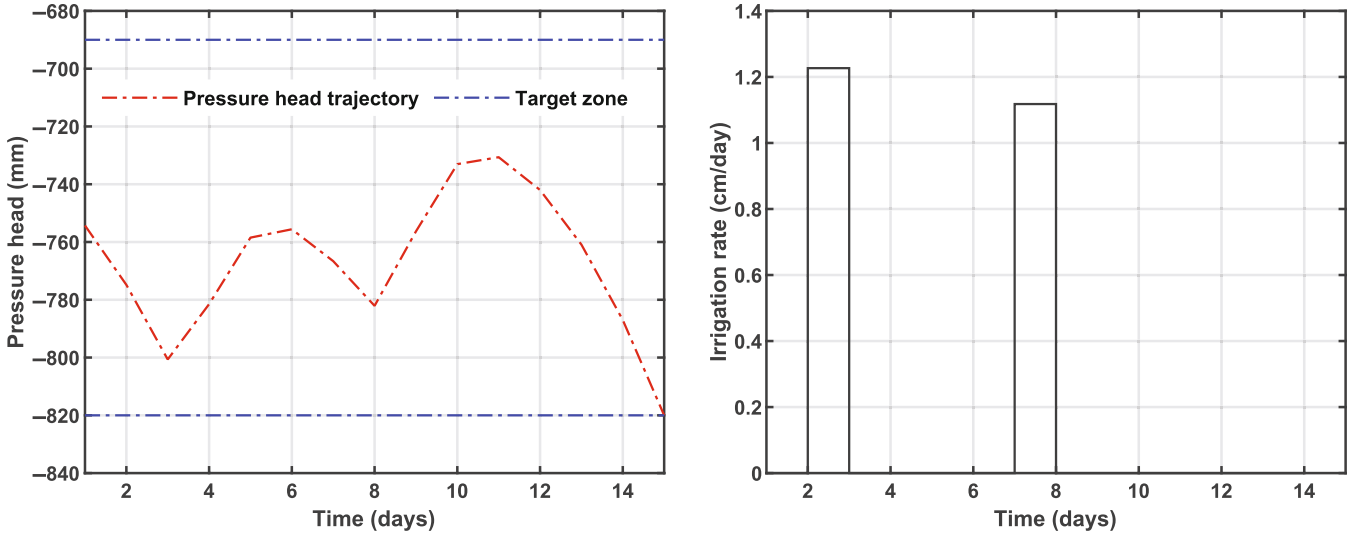

(A) Capillary pressure head. (B) Prescribed irrigation rate.

FIGURE 9 Open-loop trajectories computed by the scheduler of Equations (19a)–(19g)

compared to the mixed integer formulation $\mathbb{P}_{\text{MINLP}}(y)$. Thus, a smaller overall cost in $\mathbb{P}_{\text{SIG}}(y)$ compared to $\mathbb{P}_{\text{MINLP}}(y)$ should be construed as a failure of the sigmoid function to adequately approximate the binary elements and not the ability of the heuristic approach to provide the best possible solution (in the sense of a minimization optimization problem). It is evident form Table 3 that, in the open-loop implementation, there is a 23-fold decrease in the computation time under $\mathbb{P}_{\text{SIG}}(y)$. From these results, it can be concluded that the computational speed of the proposed scheduler is remarkably enhanced when the binary variable in $\mathbb{P}_{\text{MINLP}}(y)$ is approximated with a sigmoid function.

5.4 | Spatially variable irrigation scheduling in small-scale fields–Case Study 2

Figure 10 shows the closed-loop scheduling results for a small-scale spatially variable field that is delineated into three MZs. It is evident that the scheduler prescribes irrigation on days 2, 9, and 16 for all the three MZs. This is due to the fact that the spatially variable scheduler for small-scale fields assumes that the irrigation implementing equipment is able to irrigate all the MZs in 1 day. Thus, whenever the discrete irrigation decision is equal to 1, all the three MZs must be irrigated. In the loam MZ,

the scheduler prescribes irrigation rates of 1.20, 1.30, and 1.25 cm/day to maintain the root zone pressure head within the target zone. In the loamy sand and sandy soil MZs, the scheduler prescribes irrigation rates of 2.40, 2.50, and 2.55 cm/day to sustain the root zone pressure head in the target zone. The scheduler prescribed same irrigation rates for these MZs due to the fact that loamy sand soils and sandy soils possess similar infiltration and drainage features.

TABLE 3 Comparison between $\mathbb{P}_{\text{MINLP}}(y)$ and $\mathbb{P}_{\text{SIG}}(y)$ (open-loop)

Formulation	$\mathbb{P}_{\text{MINLP}}(\boldsymbol{y})$	$\mathbb{P}_{\text{SIG}}(\boldsymbol{y})$
Computation time (min)	57.8	2.5
Cost	106.5	106.5

5.5 | Spatially variable irrigation scheduling in large-scale fields–Case Study 3

Figure 11 shows the closed-loop scheduling results for a large-scale spatially variable field that is delineated into two MZs. In this simulation case study, the irrigation implementing equipment starts its irrigation cycle from the loamy sand MZ and completes its irrigation cycle after 2 days in the loam MZ. The loam MZ can be irrigated on days 2, 4, 6, 8, 10, 12, 14, 16, 18, and 20, while the loamy sand MZ can be irrigated on days 1, 3, 5, 7, 9, 11, 13, 15, 17, and 19. The scheduler prescribes three irrigation cycles during the 20 day simulation period. From Figure 11, it can be seen that the days that make up the 3 cycles are days 1 and 2 for the first cycle, days 9 and 10 for the second cycle, and days 17 and 18 for the third cycle. For the loamy sand MZ, the scheduler

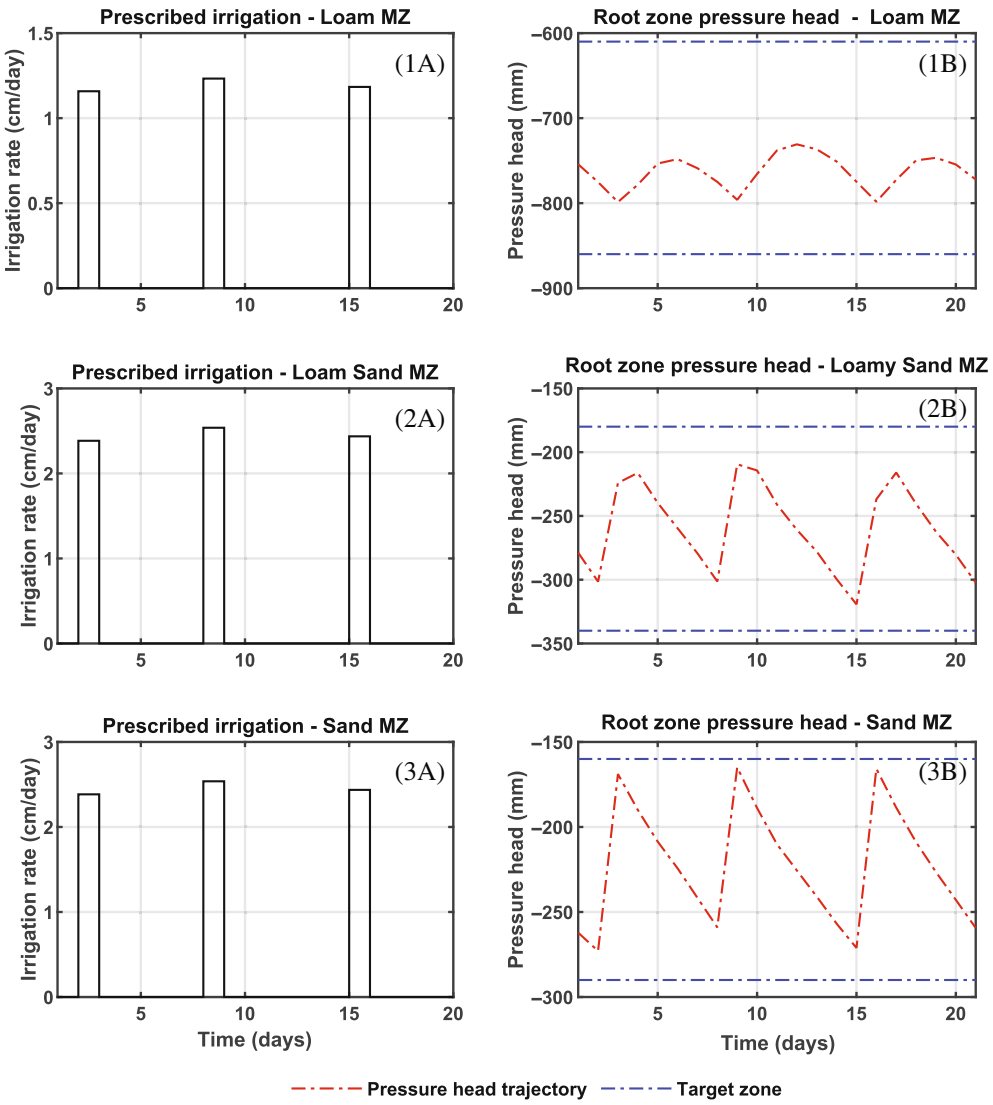

FIGURE 10 Closed-loop trajectories under the spatially variable scheduler of Equations (21b)–(21g) for (i) (1A and 1B) loam management zone, (ii) (2A and 2B) loamy sand MZ, and (iii) (3A and 3B) sand MZ

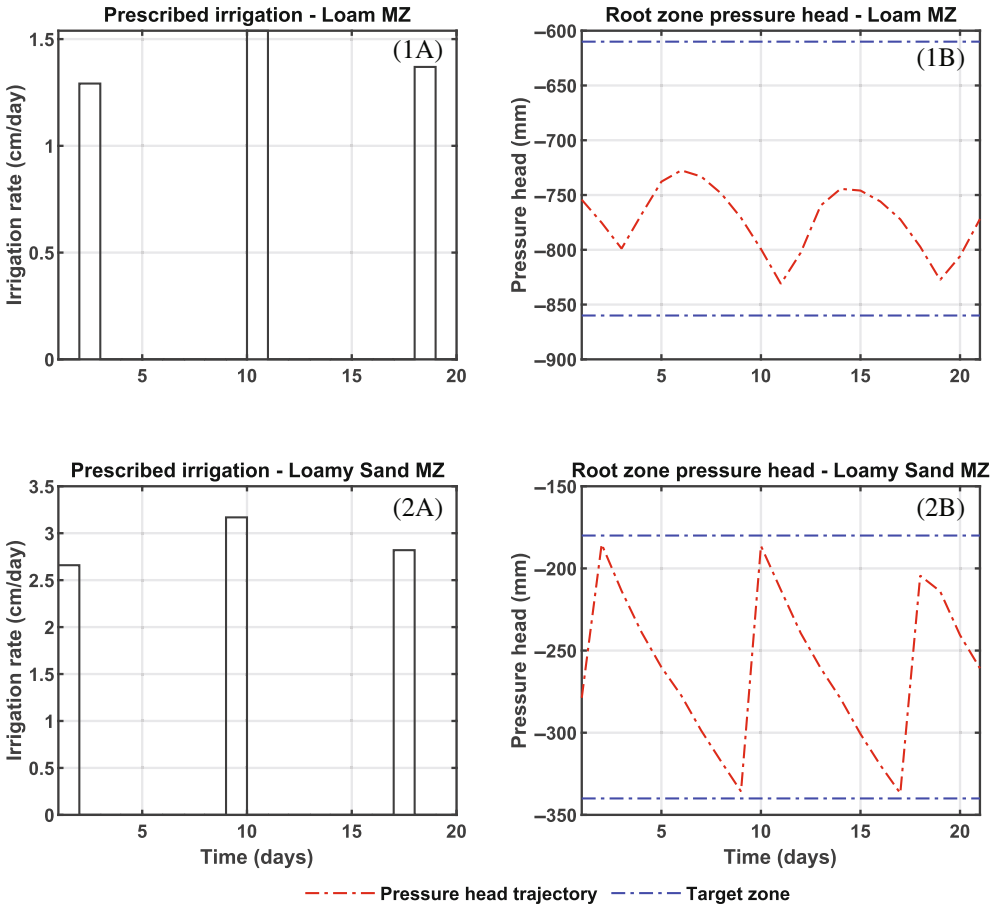

FIGURE 11 Closed-loop trajectories under the spatially variable scheduler of Equations (22a)–(22i) for (i) (1A and 1B) loam management zone (MZ), and (ii) (2A and 2B) loamy sand MZ

prescribes irrigation rates of 2.70, 3.20, and 2.75 cm/day on days 1, 9, and 17 to maintain the root zone pressure head in the target zone. For the loam MZ, the scheduler prescribes irrigation rates of 1.30, 1.50, and 1.35 cm/day on days 2, 10, and 18.

5.6 | General discussion

The validation results indicate that the proposed LSTM model framework for the agro-hydrological system is robust and accurate, supporting a number of studies that have also used LSTM models to describe the dynamics of soil moisture in the soil–crop–atmosphere system.[9,11] In previous works that have used MPC to determine irrigation schedules,[5,6,15,16] the determination of the timing of the irrigation event was done outside the MPC formulation using heuristic methods. Consequently, the determination of the irrigation time in the aforementioned works is not necessarily optimal, since heuristic approaches are not guaranteed to provide optimal solutions. In this research study, we encoded the irrigation time (day) with a binary variable and included this binary variable in the MPC formulation. This approach ensured the optimal selection of the timing of the irrigation event. Furthermore, the size of the agro-hydrological system and its attendant effect on the calculation of irrigation schedules were not considered in the MPC formulations of the earlier mentioned works. In this paper, novel MPC formulations were developed for small- and large-scale fields.

6 | SUMMARY AND CONCLUSIONS

This study examined the use of a machine learning-based MPC framework for the determination of daily irrigation schedules. The proposed irrigation scheduler will be beneficial to a wide range of fields encountered in agricultural practice, namely, small-scale, large-scale, homogeneous, and spatially variable fields. We suggested using an LSTM network to model the root zone soil moisture content in the soil-crop-atmosphere system. It was observed that by formulating the model-based scheduler as a mixed-integer MPC with zone control, the timing of the irrigation event and the irrigation rate could be determined optimally. The simulation results revealed that the LSTM model was capable of performing accurate single-step and multi-step predictions of the root zone capillary pressure head. The results from

the simulation case studies highlight the efficacy of the proposed scheduler, as it was able to prescribe irrigation schedules that are typical of irrigation practice. The proposed approach can thus be successfully used to maximize crop yield while minimizing total water consumption and irrigation costs. The heuristic method involving the sigmoid function was capable of enhancing the computational efficiency of the scheduler and this underscores the capability of the proposed approach to prescribe optimal or near-optimal irrigation schedules within workable computational budgets.

Despite these promising initial results, some near-term modifications of the proposed scheduler should be carried out to ensure more robust results. First, it is more suitable to maintain the capillary pressure head throughout the root zone, instead of at a specific depth. This suggests that the LSTM model should be trained to predict the capillary pressure head throughout the entire root zone. Additionally, because the root zone changes with space and time during the growing season, the LSTM model of the agro-hydrological system should be trained to reflect the time- and spatially-varying nature of the root zone. In this regard, other modelling approaches can also be explored. For example, local models in time and space can be developed to capture the time- and spatially-varying dynamics of the root zone. Techniques such as the sparse proper orthogonal decomposition (SPOD)-Garlerkin methods,[35] the dynamic mode decomposition with control method,[36] and the proper orthogonal decomposition[37] method can be used to develop such local models for the agro-hydrological system. Second, the resilience of the proposed scheduler to uncertainties in weather predictions should be extensively tested. In this regard, we surmise that the use of zone control in the proposed scheduler will enhance the robustness of the scheduler due to the inherent robustness of zone control. Thus, the presence of a sufficiently small uncertainty arising from imperfect weather predictions will not degrade the performance of the scheduler. In instances where a large uncertainty causes the root zone pressure to fall out of its range for a sustained period, a funnel-shaped target zone can be employed to drive the root zone pressure head back within its range. Lastly, it is a well-established notion that improved performance can be realized in industries by integrating scheduling and control. Similarly, it will be helpful to explore the benefits that may be obtained by integrating the proposed scheduling approach with closed-loop control in agro-hydrological systems. Several frameworks for integrating scheduling and control have been proposed (e.g., in the works of Cao et al. and Burnak and Pistikopoulos[38,39]). It will be important to leverage these frameworks and extend these frameworks to scheduling and control in irrigation management.

AUTHOR CONTRIBUTIONS

Bernard T. Agyeman: Data curation; formal analysis; investigation; methodology; software; validation; writing – original draft. **Soumya R. Sahoo:** Methodology; writing – review and editing. **Jinfeng Liu:** Conceptualization; funding acquisition; methodology; project administration; supervision; writing – review and editing. **Sirish L. Shah:** Funding acquisition; supervision; writing – review and editing.

ACKNOWLEDGEMENTS

Financial support from Alberta Innovates and Natural Sciences and Engineering Research Council of Canada is gratefully acknowledged.

DATA AVAILABILITY STATEMENT

Data available on request from the authors

ORCID

Jinfeng Liu https://orcid.org/0000-0001-8873-847X

REFERENCES

[1] R. Connor, *The United Nations World Water Development Report 2015: Water for a Sustainable World,* Vol. 1, UNESCO Publishing, Paris, France **2015**.
[2] M. H. Ali, M. S. U. Talukder, *J. Inst. Eng.* **2001**, *28*, 11.
[3] S. L. Shah, B. R. Bakshi, J. Liu, C. Georgakis, B. Chachuat, R. D. Braatz, B. R. Young, *AIChE J.* **2021**, *67*(2), e17113.
[4] S. O. Lopes, F. A. C. C. Fontes, R. Pereira, M. De Pinho, A. M. Gonçalves, *Math. Probl. Eng.* **2016**, *2016*, 1.
[5] Y. Park, J. S. Shamma, T. C. Harmon, *Environmental Modelling & Software* **2009**, *24*(9), 1112.
[6] J. Nahar, S. Liu, Y. Mao, J. Liu, S. L. Shah, *Ind. Eng. Chem. Res.* **2019**, *58*(26), 11485.
[7] F. Capraro, D. Patino, S. Tosetti, C. Schugurensky, in *2008 IEEE Int. Conf. on Networking, Sensing and Control*, IEEE, Sanya, China **2008**.
[8] S. W. Tsang, C. Y. Jim, *Energy and Buildings* **2016**, *127*, 360.
[9] Z. Gu, T. Zhu, X. Jiao, J. Xu, Z. Qi, *Computers and Electronics in Agriculture* **2021**, *180*, 105801.
[10] D. Brezak, T. Bacek, D. Majetic, J. Kasac, B. Novakovic, in *2012 IEEE Conf. on Computational Intelligence for Financial Engineering & Economics*, IEEE, New York **2012**.
[11] O. Adeyemi, I. Grove, S. Peets, Y. Domun, T. Norton, *Sensors* **2018**, *18*(10), 3408.
[12] N. H. Rao, P. B. S. Sarma, S. Chander, *Agricultural Water Management* **1988**, *15*(2), 165.
[13] G. Naadimuthu, K. S. Raju, E. S. Lee, *Mathematical and Computer Modelling* **1988**, *30*(7-8), 165.
[14] J. B. Rawlings, M. J. Risbeck, *Automatica* **2017**, *78*, 258.
[15] A. C. McCarthy, N. H. Hancock, S. R. Raine, *Computers and Electronics in Agriculture* **2014**, *101*, 135.
[16] D. Delgoda, H. Malano, S. K. Saleem, M. N. Halgamuge, *Environmental Modelling & Software* **2016**, *78*, 40.

[17] Z. Wu, A. Tran, D. Rincon, P. D. Christofides, *AIChE J.* **2019**, *65*(11), e16729.
[18] Z. Wu, D. Rincon, J. Luo, P. D. Christofides, *AIChE J.* **2021**, *67*(4), e17164.
[19] T. Zhao, Y. Zinghe, J. Gong, Z. Wu, *Chem. Eng. Res. Des.* **2022**, *179*, 435.
[20] C. A. Floudas, X. Lin, *Annals of Operations Research* **2005**, *139*(1), 131.
[21] D. Q. Mayne, J. B. Rawlings, C. V. Rao, P. O. M. Scokaert, *Automatica* **2000**, *36*(6), 789.
[22] B. T. Agyeman, S. R. Sahoo, J. Liu, S. L. Shah, *IFAC - Papers Online* **2022**, *55*(7), 334.
[23] S. Bo, S. R. Sahoo, X. Yin, J. Liu, S. L. Shah, *Mathematics* **2020**, *8*(1), 134.
[24] B. Majone, F. Viani, E. Filippi, A. Bellin, A. Massa, G. Toller, F. Robol, M. Salucci, *Procedia Environ. Sci.* **2013**, *19*, 426.
[25] Y. Mualem, *Water Resour. Res.* **1976**, *12*(3), 513.
[26] M. T. Van Genuchten, *Soil Sci. Soc. Am. J.* **1980**, *47*(5), 892.
[27] M. W. Farthing, F. L. Ogden, *Soil Sci. Soc. Am. J.* **2017**, *81*(6), 1257.
[28] R. A. Feddes, P. J. Kowalik, H. Zaradny, *Simulation of Field Water Use and Crop Yield*, John Wiley & Sons, New York **1982**.
[29] A. P. Mazzini, E. N. Asada, G. G. Lage, *IET Generation, Transmission & Distribution* **2018**, *12*(12), 2897.
[30] E. J. de Oliveira, I. C. Da Silva, J. L. R. Pereira, S. Carneiro, *IEEE Transactions on Power Systems* **2005**, *20*(3), 1616.
[31] F. J. Moral, J. M. Terrón, J. R. M. da Silva, *Soil Tillage Res.* **2010**, *106*(2), 335.
[32] B. A. King, R. W. Wall, L. R. Wall, *Applied Engineering in Agriculture* **2005**, *21*(5), 871.
[33] R. F. Carsel, S. R. Parrish, *Water Resour. Res.* **1988**, *24*(5), 755.
[34] S. Bo, J. Liu, *Mathematics* **2020**, *8*(5), 681.
[35] H. S. Sidhu, A. Narasingam, P. Siddhamshetty, J. S.-I. Kwon, *Comput. Chem. Eng.* **2018**, *112*, 92.
[36] A. Narasingam, J. S.-I. Kwon, *Comput. Chem. Eng.* **2017**, *106*, 501.
[37] A. Narasingam, P. Siddhamshetty, J. S.-I. Kwon, *Ind. Eng. Chem. Res.* **2018**, *57*(11), 3977.
[38] K. Cao, S. H. Son, J. Moon, J. S.-I. Kwon, *Appl. Energy* **2021**, *302*, 117487.
[39] B. Burnak, E. N. Pistikopoulos, *AIChE J.* **2020**, *66*(10), e16981.

How to cite this article: B. T. Agyeman, S. R. Sahoo, J. Liu, S. L. Shah, *Can. J. Chem. Eng.* **2023**, *101*(6), 3362. https://doi.org/10.1002/cjce.24764